

# Inelastic carrier lifetime in graphene

E. H. Hwang,<sup>1</sup> Ben Yu-Kuang Hu,<sup>2,1</sup> and S. Das Sarma<sup>1</sup>

<sup>1</sup>*Condensed Matter Theory Center, Department of Physics,  
University of Maryland, College Park, Maryland 20742-4111 and*

<sup>2</sup>*Department of Physics, University of Akron, Akron, OH 44325-4001*

(Dated: December 2, 2024)

We consider hot carrier inelastic scattering due to electron-electron interactions in graphene, as functions of carrier energy and density. We calculate the imaginary part of the zero-temperature quasiparticle self-energy for doped graphene, utilizing the  $G_0W$  and random phases approximations. Using the full dynamically screened Coulomb interaction, we obtain the inelastic quasiparticle lifetimes and associated mean free paths. The linear dispersion of graphene gives lifetime energy dependences that are qualitatively different from those of parabolic-band semiconductors. We also get good agreement with data from angle-resolved photoemission spectroscopy experiments.

PACS numbers: 81.05.Uw; 71.10.-w; 71.18.+y; 73.63.Bd

Graphene, a single layer of carbon atoms covalently bonded together in a honeycomb structure (as in a monolayer of graphite), was previously thought to be unstable and hence non-existent in a free state. Recently, however, Novoselov *et al.* reported [1] that they had succeeded in fabricating single graphene sheets. Subsequently, several experimental groups have reported interesting transport and spectroscopic measurements [2, 3], which has led to experimental and theoretical interest in this field that is rapidly burgeoning.

The overlap of the  $\pi_z$  orbitals between neighboring carbon atoms in the graphene plane is accurately described by a tight-binding Hamiltonian. Around the  $K$  and  $K'$  points (often called Dirac points) which are at the corners of the hexagonal Brillouin zone, the kinetic energy term of the Hamiltonian is well-approximated by a two-dimensional (2D) Dirac equation for massless particles,  $\hat{H}_0 = -v_0(\sigma_x \hat{k}_x + \sigma_y \hat{k}_y)$ , where  $\sigma_x$  and  $\sigma_y$  are  $2 \times 2$  Pauli spinors and  $\mathbf{k}$  is the momentum relative to the Dirac points ( $\hbar = 1$  throughout this paper). The two components of the spinors correspond to occupancy of the two sublattices of the honeycomb structure in a hexagonal lattice. This  $\hat{H}_0$  gives a linear energy dispersion relation  $\epsilon_{\mathbf{k},s} = sv_0|\mathbf{k}|$ , where  $s = +1$  ( $-1$ ) for the conduction (valence) band. The corresponding density of states (DOS) is  $D(\epsilon) = g_s g_v |\epsilon| / (2\pi v_0^2)$ , where  $g_s = 2$ ,  $g_v = 2$  are the spin and valley (*i.e.*,  $K$  and  $K'$  points) degeneracies, respectively. Thus, graphene is a gapless semiconductor. In intrinsic graphene, the Fermi level lies at the Dirac points, but as with other semiconductors it is possible to shift the Fermi level either by doping the sample or applying an external gate voltage, which introduces 2D free carriers (electrons or holes) producing extrinsic graphene with gate voltage induced tunable carrier density. The Fermi momentum ( $k_F$ ) and the Fermi energy ( $E_F$ , relative to the Dirac point energy) of graphene are given by  $k_F = (4\pi n/g_s g_v)^{1/2}$  and  $|E_F| = v_0 k_F$  where  $n$  is the 2D carrier (electron or hole) density.

Interparticle interactions can significantly affect elec-

tronic properties, particularly in systems of reduced dimensionality. Moreover, the linear energy dispersion around the Dirac points gives condensed matter experimentalists a unique opportunity to study interaction effects on effectively massless particles. In this paper, we focus on the effect of electron-electron interaction effects on the imaginary part of quasiparticle self-energies,  $\text{Im}[\Sigma]$ . From  $\text{Im}[\Sigma]$ , we can extract the quasiparticle lifetime, which gives information that is relevant both to fundamental questions, such as whether or not the system is a Fermi liquid, and to possible applications, such as the energy dissipation rate of injected carriers in a graphene-based device. In particular, an important physical quantity of both fundamental and technological significance is the hot carrier mean free path, which we calculate as a function of energy, density and in-plane dielectric constant. Furthermore,  $\text{Im}[\Sigma]$ , being the width of the quasiparticle spectral function, is related to measurements in angle resolved photoemission spectroscopy (ARPES).

The self-energy  $\Sigma$  within the leading-order ring-diagram  $G_0W$  approximation is [4]

$$\Sigma_s(\mathbf{k}, i\omega_n) = -k_B T \sum_{s'} \sum_{\mathbf{q}, i\nu_n} G_{0,s'}(\mathbf{k} + \mathbf{q}, i\omega_n + i\nu_n) \times W(\mathbf{q}, i\nu_n) F_{ss'}(\mathbf{k}, \mathbf{k} + \mathbf{q}). \quad (1)$$

Here,  $T$  is temperature,  $s, s' = \pm 1$  are band indices,  $G_0$  is the bare Green's function,  $\omega_n, \nu_n$  are Matsubara fermion frequencies,  $W$  is the screened Coulomb interaction, and  $F_{ss'}(\mathbf{k}, \mathbf{k}') = \frac{1}{2}(1 + ss' \cos \theta_{\mathbf{k}\mathbf{k}'})$ , where  $\theta_{\mathbf{k}\mathbf{k}'}$  is the angle between  $\mathbf{k}, \mathbf{k}'$ , arises from the overlap of  $|s\mathbf{k}\rangle$  and  $|s'\mathbf{k}'\rangle$ . The screened interaction  $W(\mathbf{q}, i\omega_n) = V_c(\mathbf{q})/\epsilon(\mathbf{q}, i\omega_n)$ , where  $V_c(\mathbf{q}) = 2\pi e^2/\kappa q$  is the bare Coulomb potential ( $\kappa$  =background dielectric constant), and  $\epsilon(\mathbf{q}, i\omega_n)$  is the 2D dynamical dielectric function. In the random phase approximation  $\epsilon(\mathbf{q}, i\omega_n) = 1 - V_c(\mathbf{q})\Pi_0(\mathbf{q}, i\omega_n)$ , where the irreducible polarizability  $\Pi_0$  is approximated by the bare bubble diagram [5], which gives the familiar Lindhard expression [with a modification to include the form

factor  $F_{ss'}(\mathbf{k}, \mathbf{k}')$ ]. The self-energy approximation described by Eq. (1) should be an excellent approximation for graphene since graphene is inherently a weak-coupling (or “high-density” in parabolic-band systems) 2D system [12].

After the standard analytical continuation from  $i\omega_n$  to  $\omega + i0^+$  to obtain the retarded self-energy  $\Sigma^{\text{ret}}$ , in the  $G_0W$  approximation at  $T = 0$ ,

$$\text{Im}[\Sigma_s^{\text{ret}}(\mathbf{k}, \omega)] = \sum_{s'} \int \frac{d\mathbf{q}}{(2\pi)^2} [\theta(\omega - \xi_{\mathbf{k}+\mathbf{q}, s'}) - \theta(-\xi_{\mathbf{k}+\mathbf{q}, s'})] \times V_c(q) \text{Im} \left[ \frac{1}{\varepsilon(q, \xi_{\mathbf{k}+\mathbf{q}, s'} - \omega)} \right] F_{ss'}(\mathbf{k}, \mathbf{k} + \mathbf{q}), \quad (2)$$

where  $\xi_{\mathbf{k}, s} = \epsilon_{\mathbf{k}, s} - \mu$ , is the electron energy relative to the chemical potential  $\mu$  ( $= E_F$  at  $T = 0$ ) and  $\theta$  is the Heaviside unit step function.

The inverse quasiparticle lifetime (or, equivalently, the scattering out rate)  $\Gamma_s(\mathbf{k})$  of state  $|s\mathbf{k}\rangle$  is obtained by setting the frequency in imaginary part of the self-energy to the on-shell (bare quasiparticle) energy  $\xi_{s\mathbf{k}}$ , *i.e.*  $\Gamma_s(\mathbf{k}) = 2 \text{Im}[\Sigma_s^{\text{ret}}(\mathbf{k}, \xi_{s\mathbf{k}})]$ . (The factor 2 comes from the squaring of the wavefunction to obtain the occupation probability.) The  $G_0W$  self-energy approximation used here is equivalent to the Born approximation for the scattering rate. Note that the integrand of Eq. (2) is non-zero only when  $\text{Im}[\epsilon] \neq 0$  or  $\text{Re}[\epsilon] = 0$ . These correspond to scattering off single-particle excitations and plasmons, respectively.

The self-energies and quasiparticle lifetimes of graphene and conventional parabolic-band semiconductors differ considerably. These differences can be explained with the help of Fig. 1, which shows the single-particle excitation (SPE) and injected-electron energy loss (IEEL) continua and the plasmon dispersion for a direct gapless 2D parabolic band semiconductor and for graphene. The intersections of the IEEL continua with the SPE continua and the plasmon dispersion lines indicate allowed decay processes via electron-electron interactions. In both doped parabolic-band semiconductors and graphene, an injected electron will decay via single-particle intraband excitations of electrons in the conduction band. In parabolic band semiconductors, an electron injected with sufficient kinetic energy can also decay via plasmon emissions and interband SPE (also known as “impact ionization”). On the other hand, as shown in Fig. 1(b), electrons injected into doped graphene cannot decay via plasmon emission, and the region in  $q-\omega$  where decay via interband SPE is allowed (along the straight line segment between  $\omega = v_0 k_F$  and  $v_0(k - k_F)$ , for  $k > 2k_F$ ) is of measure zero. In fact, within the Born approximation the quasiparticle lifetime of graphene due to electron-electron interactions at  $T = 0$  is infinite. (Multiparticle excitations, which are excluded in the approximations used here, will give a quasiparticle a finite lifetime [6], but this is a relatively small effect in graphene.)

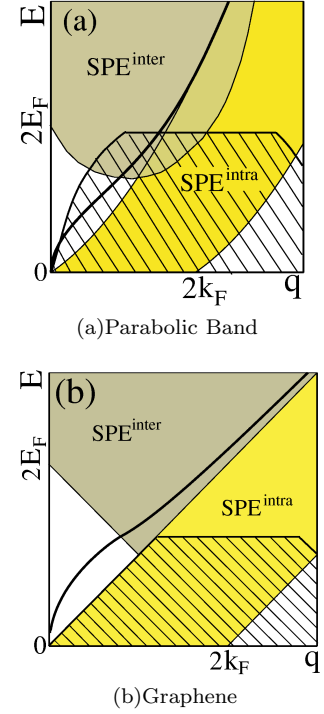


FIG. 1: The single-particle excitations (intraband and interband) and injected-particle energy-loss (hatched region) continua, and plasmon dispersion (thick line) for (a) gapless parabolic-band semiconductor with equal hole and electron masses and (b) graphene, at  $T = 0$  with Fermi energy in the conduction band. For gapped semiconductors, the interband continua are shifted up by the energy gap.

In doped graphene, the only independent parameters relevant for Born approximation quasiparticle scattering rates at  $T = 0$  are the Fermi energy relative to the Dirac point  $E_F = v_0 k_F$  and the dimensionless coupling (“interaction strength”) constant  $r_s = e^2/(\kappa v_0)$  ( $\sim$  ratio of average Coulomb potential and kinetic energies of the electrons in the conduction band) which for graphene is approximately  $(2.2)/\kappa$ , where  $\kappa$  is the effective dielectric constant of the graphene layer and the media surrounding it. The scattering rate, which has units of energy, must therefore be proportional to  $E_F$ , and must be a function only of  $\epsilon/E_F = k/k_F$  and  $r_s$ . Fig. 2(a) shows the Born approximation  $T = 0$  quasiparticle lifetime  $1/\tau = \Gamma$  due to electron-electron interactions as a function of energy  $\xi(k) = \epsilon_k - E_F$ . Since the speed of the quasiparticles close to the Dirac point is approximately a constant  $v_0 \approx 10^8 \text{ cm/s}$ , the inelastic mean free path  $\ell$  is obtained by  $\ell(\xi) = v_0 \tau(\xi)$ . In inset of Fig. 2(a), we provide the corresponding  $\ell$ , which shows that at  $n = 10^{13} \text{ cm}^{-2}$  a hot electron injected with an energy of 1 eV above  $E_F$  has an  $\ell$  due to electron-electron interactions that is on the order of 20 nm. This will have implications for designing any hot electron transistor type graphene devices.

As with doped parabolic-band semiconductors, in

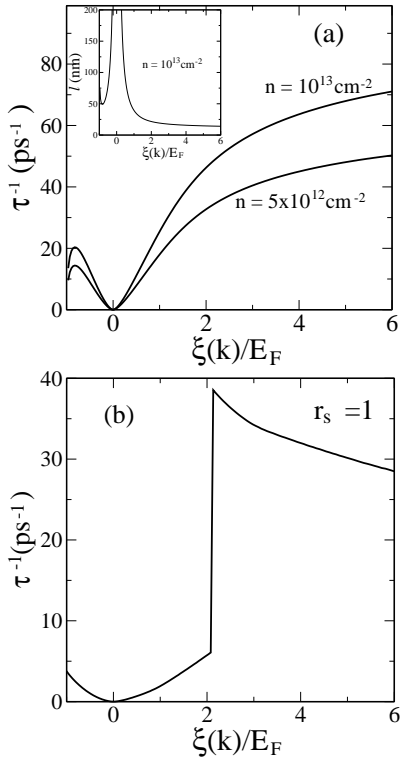


FIG. 2: (a) Inelastic quasiparticle lifetime/scattering rate ( $1/\tau = \Gamma$ ) in graphene due to dynamically screened electron-electron interactions, as a function of energy at  $T = 0$  for different densities, within the Born approximation. Inset shows the corresponding quasiparticle mean free path for  $n = 10^{13} \text{ cm}^{-2}$  (corresponding to  $E_F \approx 0.4 \text{ eV}$ ). (b) Equivalent scattering rate for a parabolic band semiconductor (without interband processes), for comparison.

graphene  $\Gamma(k) = 1/\tau(k) \propto (k - k_F)^2$  for  $k \approx k_F$  due to scattering phase-space restrictions. Further away from  $k_F$ , however, the dependence of  $\Gamma$  on  $k$  in graphene and in parabolic-band semiconductors are markedly and qualitatively different. To wit, in parabolic band semiconductors plasmon emission [7, 8] and interband collision thresholds [9] cause discontinuities in the  $\Gamma(k)$ , as shown in Fig. 2(b), but the graphene  $\Gamma(k)$  is a smooth function because both plasmon emission and interband processes are absent.

In order to see the effects of the plasmons and interband SPE in graphene in  $\text{Im}[\Sigma^{\text{ret}}]$ , one must look *off*-shell, *i.e.*,  $\omega \neq \xi_{\mathbf{k},s}$ . The off-shell  $\text{Im}[\Sigma_s^{\text{ret}}]$  is not merely of academic interest; it is needed to interpret data from ARPES. The spectra of the ARPES electrons ejected from graphene give the electronic spectral function, from which one can infer  $\Sigma_s^{\text{ret}}(\mathbf{k}, \omega)$  [10]. Physically, in the  $G_0W$  approximation, the off-shell  $2\text{Im}[\Sigma_s^{\text{ret}}(\mathbf{k}, \omega)]$  gives the Born approximation decay rate of the quasiparticle in state  $\mathbf{k}$  if it had kinetic energy  $\omega + E_F$  rather than  $\xi_{\mathbf{k}} + E_F$ .

In Fig. 3 we show  $\text{Im}[\Sigma_s^{\text{ret}}(\mathbf{k}, \omega)]$  for  $k = 0$  and  $k = k_F$

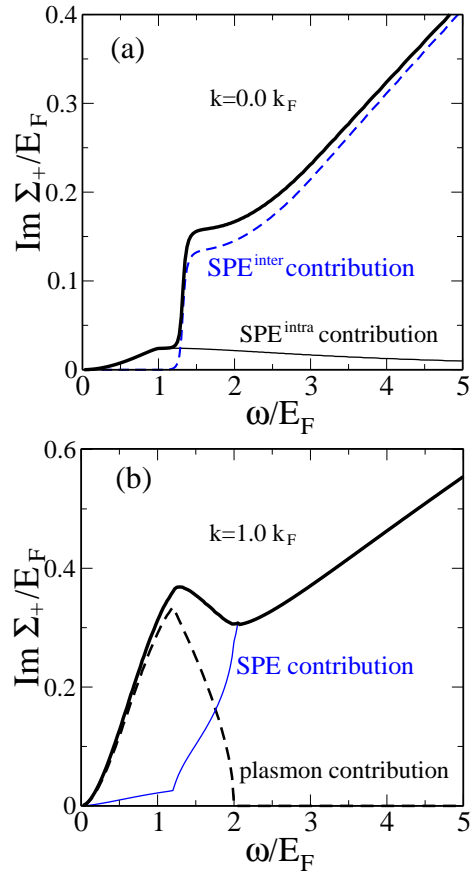


FIG. 3: The imaginary part the retarded self-energy at  $T = 0$  (thick line) for (a)  $k = 0$  and (b)  $k = k_F$  as a function of energy. The thin solid and dashed lines in (a) are the SPE<sup>intra</sup> and SPE<sup>inter</sup> contributions, respectively. The thin solid and the dashed lines in (b) are the total SPE (intraband and interband SPE) and the plasmon contributions, respectively.

as a function of  $\omega$ . Within the  $G_0W$  approximation, the contributions to the off-shell  $\text{Im}[\Sigma_s^{\text{ret}}(\mathbf{k}, \omega)]$  can be visualized as the intersection of the SPE continuum and plasmon line in Fig. 1 with the vertically displaced IEEL [11]. At  $k = 0$  there are two contributions to  $\text{Im}[\Sigma]$ , the intraband and interband SPEs. For low energies ( $|\omega| \lesssim E_F$ ) only intraband SPE contributes to  $\text{Im}[\Sigma]$ . Its contribution reaches a maximum around Fermi energy, then decreases gradually with increasing energy, as is the case with a parabolic-band semiconductor [7] where it is the only decay channel for the quasiparticle (assuming  $\omega <$  band gap energy). But in graphene there is a new decay channel of the quasiparticle, the interband SPE. Due to the phase space restrictions the interband SPE does not contribute to the self energy at low energies, but at higher energies ( $\omega \gtrsim E_F$ ) its contribution increases sharply, overwhelming the SPE<sup>intra</sup> contribution. The SPE<sup>inter</sup> contribution then increases almost linearly with  $\omega$ , with the same slope as for intrinsic graphene [12]. Plasmons do not contribute to  $\text{Im}[\Sigma_+^{\text{ret}}(\mathbf{k} = 0, \omega)]$  for  $\omega > 0$ .

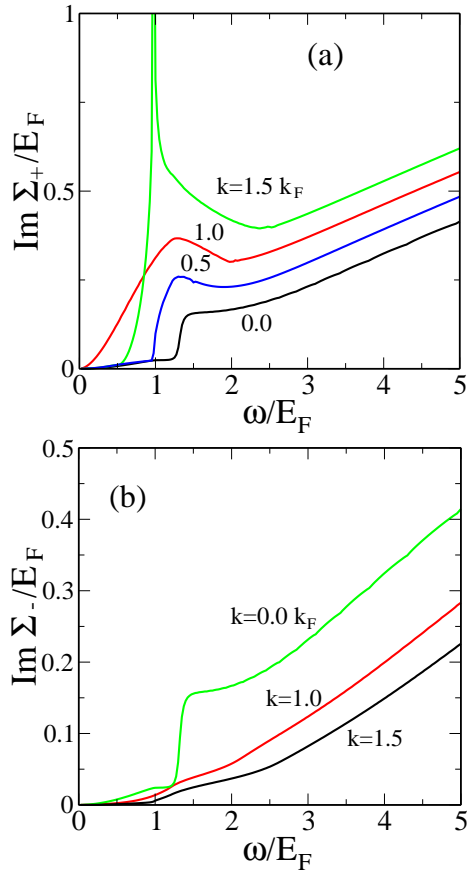


FIG. 4: The imaginary part of the self energy as a function of energy for wavevectors  $k = 0, 0.5, 1.0, 1.5k_F$  for (a) the conduction band and (b) the valence band of electron-doped graphene at  $T = 0$ .

At  $k = k_F$ , not only do plasmons contribute to  $\text{Im}[\Sigma]$ , in the low-energy ( $\omega \lesssim 2E_F$ ) regime, they actually dominate over the SPE contributions, as can be seen in Fig. 3(b). In contrast, in parabolic-band 2DEGs the plasmon and SPE contributions to  $\text{Im}[\Sigma^{\text{ret}}(k_F, \omega)]$  go as  $\omega^2$  and  $\omega^2 \ln \omega$ , respectively [8], and hence both contributions are roughly equal in magnitude.

Fig. 4 shows the imaginary part of the quasiparticle self-energies for the conduction band,  $\text{Im}[\Sigma^{\text{ret}}]$ , and the valence band,  $\text{Im}[\Sigma^{\text{ret}}]$ , of graphene for several different wavevectors. For  $k > k_F$ , the  $\text{Im}[\Sigma^{\text{ret}}]$  shows a sharp peak associated with the plasmon emission threshold. In the high energy regime, the dominant contribution to  $\text{Im}[\Sigma]$  comes from the interband SPE, which gives rise to an  $\text{Im}[\Sigma]$  is linear in  $\omega$  for all wavevectors. Note that within the  $G_0W$  approximation, for a given  $r_s$  in graphene, the  $\Sigma$ ,  $\omega$  and  $k$  scale with  $E_F$ ,  $E_F$  and  $k_F$ , respectively; *i.e.*, for fixed  $r_s$ , the function  $\tilde{\Sigma}(\tilde{k}, \tilde{\omega})$  is universal, where  $\tilde{\Sigma} = \Sigma/E_F$ ,  $\tilde{k} = k/k_F$  and  $\tilde{\omega} = \omega/E_F$ .

Finally, Fig. 5 shows the calculated  $\text{Im}[\Sigma^{\text{ret}}]$  at fixed  $k = k_F$  as a function of energy  $\omega$  for various densities. *No fitting parameters were used* in this calcula-

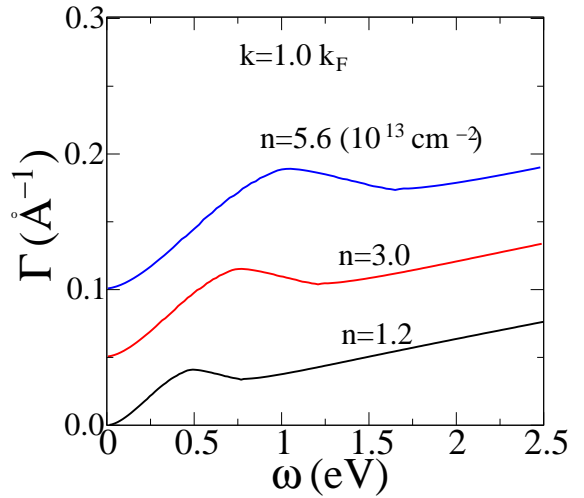


FIG. 5: Scattering rate as a function of energy for different densities,  $n = 1.2, 3.0, 5.6 \times 10^{13} \text{ cm}^{-2}$  (for clarity, successive lines are shifted upward by  $0.05 \text{ \AA}^{-1}$ ), in the form of Fig. 3 of Bostwick *et al.* [3].

tion. These results compare favorably with the recent data from ARPES experiments by Bostwick *et al.* [3] from which they extract  $\text{Im}[\Sigma(k_F, \omega)]$  for different densities. Bostwick *et al.* make the assumption that the  $\Sigma(k, \omega)$  is approximately independent of wavevector for  $k$  around  $k_F$ . We have verified that this is indeed true for  $0.8k_F \lesssim k \lesssim 1.2k_F$ . Note that the energy dependence of  $\text{Im}[\Sigma(k_F, \omega)]$  comes entirely from the SPE and plasmon contributions [see Fig. 3(b)] due to the electron-electron interaction. We find that, contrary to Bostwick *et al.*'s interpretation of their own data [3], phonon effects do not need to be included to obtain good theoretical agreement with their results.

To conclude, we have calculated the electron-electron interaction induced hot electron inelastic scattering in graphene, finding a number of intriguing and significant differences with the corresponding 2D parabolic dispersion systems. Our infinite ring-diagram  $G_0W$  approximation should be an excellent quantitative approximation for graphene since graphene is a low- $r_s$  (*i.e.*, weak-coupling) system. The Fermi temperature  $T_F$  in graphene being very high at typical densities ( $T_F \approx 3.1 \times 10^3 \text{ K}$  for  $n = 10^{13} \text{ cm}^{-2}$ , and  $T_F \propto \sqrt{n}$ ), our  $T = 0$  results should remain valid at these densities all experimental temperatures. We obtain good agreement with recent ARPES data without invoking any phonon effects.

This work is supported by US-ONR.

---

[1] K. S. Novoselov *et al.*, Science **306**, 666 (2004); Nature **438**, 197 (2005).  
[2] See *e.g.*, C Berger *et al.*, J. Phys. Chem. B **108**, 19912

(2004); Y. Zhang *et al.*, *Nature* **438**, 201 (2005); J. S. Bunch *et al.*, *Nano Lett.* **5**, 2887 (2005); A.C. Ferrari *et al.*, *Phys. Rev. Lett.* **97**, 187401 (2006) and references therein.

[3] A. Bostwick, T. Ohta, T. Seyller, K. Horn, and E. Rotenberg, cond-mat/0609660.

[4] See, *e.g.*, G.D. Mahan, *Many Particle Physics*, 3rd ed. (Kluwer/Plenum, New York, 2000).

[5] E. H. Hwang and S. Das Sarma, cond-mat/0610561.

[6] J. Gonzalez, F. Guinea, and M. A. H. Vozmediano, *Phys. Rev. Lett.* **77**, 3589 (1996).

[7] R. Jalabert and S. Das Sarma, *Phys. Rev. B* **40**, 9723 (1989).

[8] G. F. Giuliani and J. J. Quinn, *Phys. Rev. B* **26**, 4421 (1982); L. Zheng and S. Das Sarma, *Phys. Rev. B* **53**, 9964 (1996).

[9] L. V. Keldysh, *zh. Eksp. Teor. Fiz.* **48**, 1692 (1965); [Sov. Phys. – JETP **21**, 1135 (1965)].

[10] For a review of ARPES, see A. Damascelli, Z. Hussain and Z.-X. Shen, *Rev. Mod. Phys.* **75**, 473 (2003).

[11] More accurately, the contributions come from the regions in the  $E$ - $q$  plane between  $E = 0$  and  $E = \omega$  in which the SPE and plasmon lines intersect with the energy loss *and* gain spectrum that is shifted along the  $E$ -axis by  $\omega - \xi_k$ .

[12] S. Das Sarma, E. H. Hwang, and W. K. Tse, cond-mat/0610581.